

# O,N-Bidentate Ruthenium Azo Complexes as Catalysts for Olefin Isomerization Reactions

Fu Ding,<sup>[a,bl]</sup> Yaguang Sun,<sup>[bl]</sup> and Francis Verpoort\*<sup>[a]</sup>

**Keywords:** Isomerization / Olefins / Ruthenium

A series of ruthenium complexes [( $\eta^6$ -*p*-cymene)RuCl(L)] [ligands L incorporate an azo group (1–5) or an imino group (6–7)] have been synthesized and studied as olefin isomerization catalyst with allylbenzene and 1-octene as model substrates. Temperature and catalyst/substrate mol ratio have been

taken into account as parameters to optimize the isomerization reaction conditions. By using <sup>1</sup>H, <sup>13</sup>C NMR, FT-IR and microanalysis, the new complexes have been characterized and the molecular structure of complex 4 has been determined by crystal structure determination.

## Introduction

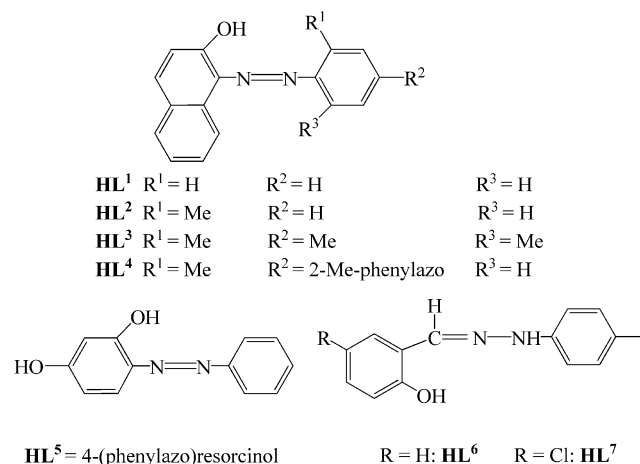
Olefin isomerization with transition-metal catalysts is well established in organic chemistry in terms of both academic curiosities and industrial interests.<sup>[1]</sup> Today, the available catalysts have proven their value in many conditions, some of them are even frequently used, for example, the Wilkinson catalyst [(PPh<sub>3</sub>)<sub>3</sub>RhCl] is employed in the isomerization of allylic ethers.<sup>[2]</sup> However, there is still a high request for cheaper, readily available and highly selective transition metal systems. Furthermore, systems providing especially mild and efficient conditions are required ensuring the C=C bond is only isomerized to a certain position.

During recent years the chemistry of half-sandwich ( $\eta^6$ -arene)ruthenium(II) complexes has been the subject of intense research in the field of organometallic chemistry.<sup>[3–6]</sup> Except for isomerization, the catalytic properties of these complexes have been investigated in various fields ranging from hydrogen transfer<sup>[7–11]</sup> to ring-closing metathesis,<sup>[4,12–14]</sup> etc.

The extension of the catalytic activities towards isomerization depends on the metal itself and its structure. Tuning of the ligand environment with the aim to develop catalysts for the isomerization is of our concern. Herein, as an addition of previous investigations on the ruthenium Schiff base chemistry,<sup>[15]</sup> analogous ligands e.g. Sudan compounds are selected as ligands to investigate.

The interest for these ligands (Scheme 1) is mainly based on three reasons. Firstly, because of the  $\pi$ -acidic nature of the azo function, the ligands are able to form M–C bonds

or metallacycles.<sup>[16]</sup> Moreover, the azo group (–N=N–) can stabilize ruthenium in lower oxidation states due to its strong  $\pi$ -acidic character, while naphtholate/phenolate oxygen, being a hard base, stabilizes the higher oxidation states of the metal ion.<sup>[15]</sup>



Scheme 1. Structure of the azo and imino ligands.

Secondly, the naphthol-based ligands are not only potential ligands that can coordinate with the metal by oxygen and nitrogen in a bidentate mode, but they are also better electron-donating agents and provide more steric crowding compared to the phenyl group. Naphthol based azo compounds have not been used very often as ligands, although recent work has gone some way to redress the balance. Until now, only three reports could be found in respect to these ligands in combination with Ru(II)<sup>[17]</sup> and Ru(III).<sup>[18,19]</sup> Two reports describe the ligands as mono-anionic O,N-bidentate donor ligands, while the third report describes the ligand as a di-anionic C,O,N-tridentate donor ligand.

[a] Department of Inorganic and Physical Chemistry, Division of Organometallics and Catalysis, Ghent University, Krijgslaan 281-S3, 9000 Ghent, Belgium  
 Fax: +32-9-264-49-83  
 E-mail: francis.verpoort@ugent.be

[b] Laboratory of Coordination Chemistry, Shenyang Institute of Chemical Technology, Shenyang 110142, P. R. China

Thirdly, we expect that some of the selected ligands can act as a tridentate donor capable of generating an extra vacancy on the metal center during the catalytic reaction.

As reported earlier in the literature, azonaphthol and azophenyl complexes have been extensively used as catalysts for transfer hydrogenation of ketones.<sup>[17,20]</sup> Among the different metals catalyzing this reaction, ruthenium-based systems are found to be effective.<sup>[21–23]</sup> However, in many cases, double bond isomerization occurs as an undesired side reaction with the result that two reactions can be performed by the same catalyst.<sup>[24–26]</sup>

In this study we focused on the synthesis, characterization and isomerization performance of half-sandwich ruthenium azo and imino complexes. To the best of our knowledge, this is the first time these compounds are studied as isomerization catalysts.

## Results and Discussion

### Synthesis

A series of ruthenium(II) complexes of the general formula  $[(\eta^6\text{-}p\text{-cymene})\text{RuCl}(\text{L}^n)]$  ( $n = 1\text{--}7$ ) incorporating an azo group (**1–5**) or an imino group (**6–7**) have been synthesized conveniently in the following way. To a solution of  $[(\eta^6\text{-}p\text{-cymene})\text{RuCl}_2]_2$  in THF, the appropriate thallium salt ( $\text{TlL}^n$ ) was added and stirred for 6–8 h at room temperature. Thallium chloride was removed via filtration. After purification, the novel ruthenium complexes were obtained as red-brown to dark-brown solids with 90–98% yield.

It follows that all ligands act as bidentate ligands, although some ligands, especially ligand **4** have been assumed to act as a tridentate N,N,O donor ligand; this was not the case here. All the complexes are found to be air-stable in both solid and liquid states at room temperature and are non-hygroscopic.

### Characterization

For ruthenium compounds, the methyl signal (singlet) of the *p*-cymene ligand appears in the range of 2.18–2.96 ppm and the isopropyl protons of the *p*-cymene ligand give rise to signals (two doublets) in the range of 1.05–1.97 ppm. The isopropyl CH signal appears as a septet in the range of 2.17–3.90 ppm. The signals of *p*-cymene ring show as either four doublets (4 H) or two doublets (2 H) and a singlet (2 H) in the range of 3.75–5.51 ppm. In  $^{13}\text{C}$  NMR spectra, the *p*-cymene resonances are assignable to four distinctive ranges of 17.63–19.08, 21.52–23.67, 29.71–31.15 and 77.94–101.80 ppm. The other spectral features are as expected. In complexes **1–7**, a similar peak in the range of 161.76–165.36 ppm corresponds to the phenolato/naphtholato C atoms.

The IR bands from the azo group of the metal complexes  $[(\eta^6\text{-}p\text{-cymene})\text{RuCl}(\text{L}^n)]$  ( $n = 1\text{--}5$ ) are most useful to determine the coordination mode. For instance, all of them exhibit

many sharp and strong vibrations within the region of 500–1700  $\text{cm}^{-1}$ . To confirm the ligand coordination IR spectra of the ligands were analyzed and compared with the spectra of the complexes. The infrared spectra of the ligands show bands around 1446–1476  $\text{cm}^{-1}$  and 1266–1278  $\text{cm}^{-1}$  corresponding to the azo group  $\nu_{\text{N}=\text{N}}$  and the aromatic  $\nu_{\text{C}=\text{O}}$  stretch vibrations respectively. In the coordinated compounds, the azo vibration,  $\nu_{\text{N}=\text{N}}$ , exposes peaks at lower frequency 1364–1380  $\text{cm}^{-1}$ . This supports the assumption that the coordination of the nitrogen atom can reduce the electron density in the azo frequency due to the  $(d\text{-}\pi) \text{Ru}^{\text{II}} \rightarrow \pi^*(\text{L})$  back bonding effect.<sup>[27]</sup> Meanwhile, in all the compounds, a shift to higher frequency occurs for the aromatic  $\nu_{\text{C}=\text{O}}$  stretch confirming the coordination of the aromatic oxygen.<sup>[19]</sup>

### X-ray Crystallography

In order to determine the coordination mode of the ligands in the ruthenium complexes and the stereochemistry of the complexes, the crystallization of the complex  $[(\eta^6\text{-}p\text{-cymene})\text{RuCl}(\text{L}^4)]$  (**4**) was performed by slow evaporation of a MeOH/hexane solution at 0–4 °C. It follows from X-ray analysis that one MeOH molecule (solvent) is enclosed in the  $[(\eta^6\text{-}p\text{-cymene})\text{RuCl}(\text{L}^4)] \cdot \text{CH}_3\text{OH}$  crystal. The X-ray analysis results and refinements are given in Tables 1 and 2. The complex essentially has an octahedral coordination geometry, as shown in Figure 1. The molecular structure shows that the  $\text{O}_1, \text{N}_2$  donor in the arylazo-naphtholate ligand adopts a bidentate chelating mode and the *p*-cymene carbons occupy one face of the octahedron. The Ru–C(arene) distances vary considerably from 2.182–2.212 Å. Compared with earlier reported work, the distances of Ru<sub>1</sub>–O<sub>1</sub>, Ru<sub>1</sub>–N<sub>2</sub> and Ru<sub>1</sub>–C are within the normal range.<sup>[17]</sup> A six-membered ring planar with the naphtholate ligand is generated by the two carbon atoms from the naphtholate

Table 1. Crystal data and structure refinement for  $[(\eta^6\text{-}p\text{-cymene})\text{RuCl}(\text{L}^4)] \cdot \text{CH}_3\text{OH}$ .

Molecular formula	$\text{C}_{35}\text{H}_{37}\text{ClN}_4\text{O}_2\text{Ru}$
Molecular weight	682.21
Crystal size [mm]	$0.18 \times 0.16 \times 0.10$
Color	brown
Crystal system	monoclinic
Space group	$P2(1)/n$
$a$ [Å]	15.845(3)
$b$ [Å]	14.337(3)
$c$ [Å]	17.406(4)
$\beta$	116.27(3)
$V$	3545.8(12)
$Z$	4
$D_c$	1.278
$F(000)$	1408
Absorption correction $T_{\text{max}}/T_{\text{min}}$	0.9469/0.9073
Goodness-of-fit on $F^2$	1.139
Absorption coefficient [ $\text{mm}^{-1}$ ]	0.551
Largest diff. peak and hole [ $\text{e} \cdot \text{Å}^{-3}$ ]	0.667/–0.629
Data/restraints/parameters	6189/326/452
$R_1, wR_2 [I > 2\sigma(I)]$	0.0993, 0.2325
$R_1, wR_2$ (all data)	0.1324, 0.2548

group, the two nitrogen atoms from the coordinated diazo group, the oxygen from the phenolic group and ruthenium. The dihedral angle of the naphthalene plane and the benzene plane C<sub>21</sub>–C<sub>26</sub> in the arylazo-naphtholate ligand is 64.0°. Comparing the crystal data with the one reported by Rakesh, most of the bond angles of the crystal  $[(\eta^6-p\text{-cymene})\text{RuCl}(\text{L}^4)]\cdot\text{CH}_3\text{OH}$  were larger due to the increased steric congestion around the Ru center.

Table 2. Selected bond lengths [Å] and angles [°] for complex **4**.

Bond lengths [Å]			
Ru(1)–O(1)	2.038(4)	Ru(1)–N(2)	2.051(5)
Ru(1)–C(4)	2.181(5)	Ru(1)–C(6)	2.183(5)
Ru(1)–C(7)	2.191(6)	Ru(1)–C(5)	2.202(6)
Ru(1)–C(3)	2.205(5)	Ru(1)–C(2)	2.211(6)
Ru(1)–Cl(1)	2.4095(15)	O(1)–C(11)	1.308(6)
Bond angles [°]			
O(1)–Ru(1)–N(2)	88.9(2)	C(4)–Ru(1)–C(6)	66.8(2)
O(1)–Ru(1)–C(4)	88.39(19)	N(2)–Ru(1)–C(5)	116.3(2)
O(1)–Ru(1)–C(6)	122.2(2)	N(2)–Ru(1)–C(2)	121.8(3)
N(2)–Ru(1)–C(4)	153.8(2)	N(2)–Ru(1)–Cl(1)	84.16(15)
N(2)–Ru(1)–C(6)	92.98(19)	C <sup>0</sup> –Ru(1)–Cl(1)	128.33(19)
N(2)–Ru(1)–C(7)	95.7(2)	C <sup>0</sup> –Ru(1)–O(1)	125.62(12)
N(2)–Ru(1)–C(3)	159.8(3)	C <sup>0</sup> –Ru(1)–N(2)	129.97(13)
O(1)–Ru(1)–Cl(1)	85.16(11)		

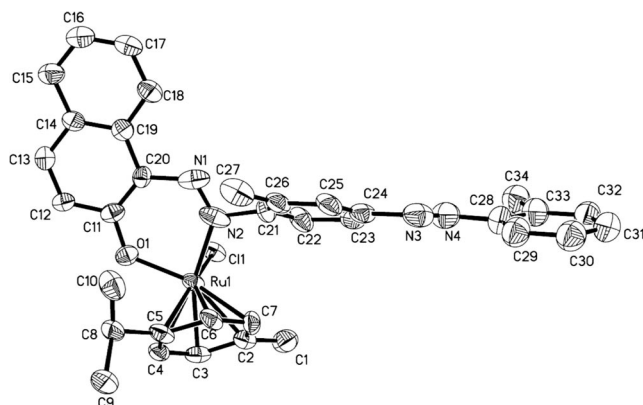


Figure 1. Molecular structure of complex **4**, the solvent molecule MeOH has been omitted for clarity (30% thermal probability ellipsoids).

### Isomerization Activity

Allylbenzene is used as a model substrate for the isomerization applying all kinds of catalysts, such as the transition metals Ti, Zr,<sup>[28]</sup> Co,<sup>[29]</sup> Rh,<sup>[30,31]</sup> Ir,<sup>[32]</sup> Au,<sup>[33]</sup> and Ru,<sup>[34–37]</sup> or Mg.<sup>[38]</sup> or even a non-metal compound like P.<sup>[39]</sup> While 1-octene is also extensively used as a model substrate,<sup>[58]</sup> these two compounds are selected as representatives alkenes to evaluate the performance of the complexes  $[(\eta^6-p\text{-cymene})\text{RuCl}(\text{L}^n)]$  ( $n = 1-7$ ).

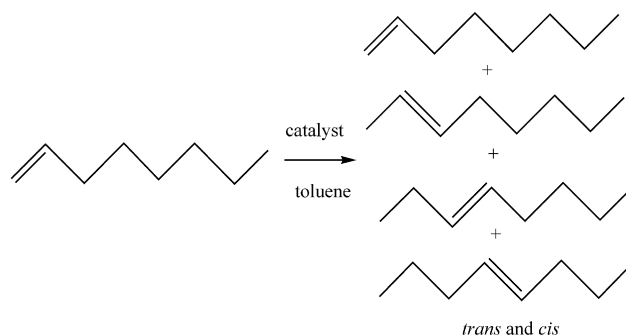
To investigate the catalytic activity, all ligands and precursor complexes have been screened under identical reaction conditions and no isomerization activity could be observed. Compound **6** and **7** are also found to be totally inactive for the isomerization of both substrates.

To optimize the reaction conditions, the different catalyst/substrate mol ratios and temperature were chosen as parameters and the results are summarized in Table 3 (Scheme 2) and Table 4 (Scheme 3).

Table 3. Isomerization of 1-octene by  $[(\eta^6-p\text{-cymene})\text{RuCl}(\text{L}^n)]$  ( $n = 1-5$ ). Conversions (substrate) and yields (products) were measured after 12 h.

Cat.	<i>T</i> [°C]	C/S <sup>[a]</sup>	% Conv. 1-octene	% Yield 2-octene	% Yield 3-octene	% Yield 4-octene <sup>[b]</sup>	
						<i>trans</i>	<i>cis</i>
<b>1</b>	60	a	90.6	14.9	49.8	0	25.8
		b	87.9	51.0	28.2	1.2	7.5
	80	a	87.0	10.5	55.4	3.5	17.6
		b	75.6	14.0	51.0	1.6	8.9
	100	a	80.4	10.0	11.3	2.1	57.0
		b	68.8	10.0	46.0	2.5	10.3
<b>2</b>	60	a	68.8	42.4	17.4	0	9.0
		b	59.8	59.7	0.1	0	0
	80	a	92.2	8.3	51.1	6.9	25.6
		b	78.7	9.5	59.0	3.2	7.0
	100	a	86.9	7.3	55.6	4.5	19.5
		b	84.2	6.7	55.5	4.2	17.9
<b>3</b>	60	a	37.6	5.9	27.3	0.6	3.9
		b	36.0	3.8	28.1	0.5	3.6
	80	a	92.2	8.2	52.4	7.1	24.5
		b	78.8	9.4	59.1	3.2	7.0
	100	a	87.1	7.2	55.7	4.6	19.6
		b	84.2	6.6	55.5	4.2	17.9
<b>4</b>	60	a	44.6	8.3	31.6	0.3	4.4
		b	27.8	3.4	21.0	0.51	2.9
	80	a	82.2	8.8	51.2	4.52	16.8
		b	73.7	10.4	51.7	1.67	10.1
	100	a	74.1	10.8	51.1	1.99	10.2
		b	56.9	6.9	42.7	1.32	6.0
<b>5</b>	60	a	32.1	4.7	24.0	0.93	2.4
		b	0.8	0.1	0.2	0.07	0.4
	80	a	1.4	0.2	0.6	0.06	0.5
		b	1.3	0.2	0.5	0.09	0.5
	100	a	1.2	0.2	0.5	0.06	0.5
		b	0.7	0.1	0.2	0.04	0.4

[a] Catalyst/Substrate (C/S) ratio: *a* = 1:1000, *b* = 1:2000. [b] GC results, only *trans/cis*-4-octene can be specified; the *trans/cis* isomers of 2- and 3-octene were not separated.



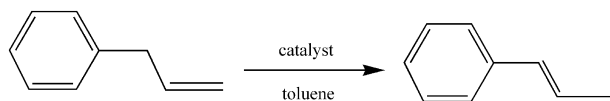
Scheme 2. Isomerization of 1-octene.

From Tables 3 and 4 it follows that changing the C/S ratio from 1:1000 to 1:2000, the reaction still proceeds smoothly accompanied by a moderate drop in conversion. Compared with the raise of the C/S ratio, the decrease of conversion is much less than half in most cases. Higher catalyst concentrations favored the formation of the *cis*-alkene;

Table 4. Isomerization of allylbenzene by  $[(\eta^6\text{-}p\text{-cymene})\text{RuCl}(\text{L}^n)]$  ( $n = 1\text{--}5$ ); conversions were measured after 12 h.

Catalyst	C/S ratio <sup>[a]</sup>	% Conversion		
		60 °C	80 °C	100 °C
$[(\eta^6\text{-}p\text{-Cymene})\text{RuCl}(\text{L}^1)]$	a	89.2	95.6	98.4
	b	73.0	93.4	96.3
$[(\eta^6\text{-}p\text{-Cymene})\text{RuCl}(\text{L}^2)]$	a	27.2	90.9	86.3
	b	25.4	85.9	70.2
$[(\eta^6\text{-}p\text{-Cymene})\text{RuCl}(\text{L}^3)]$	a	10.8	90.8	86.2
	b	10.1	85.9	70.1
$[(\eta^6\text{-}p\text{-Cymene})\text{RuCl}(\text{L}^4)]$	a	34.1	81.1	76.9
	b	27.6	66.5	31.5
$[(\eta^6\text{-}p\text{-Cymene})\text{RuCl}(\text{L}^5)]$	a	6.5	5.7	3.4
	b	2.3	1.6	0.4

[a] Catalyst/substrate molar ratios:  $a = 1:1000$ ,  $b = 1:2000$ .



Scheme 3. Isomerization of allylbenzene.

as the catalyst concentration was lowered, more *trans*-isomer was formed. Comparing the different catalysts it follows that the variation in selectivity is related to the bulkiness of the aniline part of the azonaphthol ligand. This signifies that less steric hindering in the *ortho* positions generates a higher *cis* ratio.

Catalysts **2–4** show higher activities when temperature is enhanced from 60–80 °C. Increasing the temperature to 100 °C diminished the final conversion. From these results, it is clear that a temperature of 80 °C is the best compromise for catalysts **2–4**.

With 1-octene as substrate, the higher the temperature, the lower the substrate conversion becomes for catalyst **1** and **5**. This phenomenon can be related to the thermal stability of the catalysts. While using allylbenzene, the behavior of catalyst **1** is consistent with the temperature, however, a contrasting behavior of catalyst **5** is observed.

If only the conversion of 1-octene is taken into account, the catalytic activity of catalysts **1–3** is similar (yield 92–90%) without dimerization or polymerization. Considering the selectivity, catalysts **1–4** all catalyze 1-octene to *n*-octene in yields higher than 50% by controlling the C:S ratio, temperature and reaction time. For the catalyst **2**, using a C:S = 1:2000, preferentially 2-octene was generated and the highest product selectivity was reached.

Comparison of the catalysts reveals that catalyst **1** has a better performance for allylbenzene, implicating an excellent yield (more than 98%) and a high selectivity (*trans*- $\beta$ -methylstyrene exclusively). Contrary to the results from late transition metal complexes in which the isomerized products are in equilibrium, this interesting result – no *cis*- $\beta$ -methylstyrene – indicates the lack of *cis/trans*-isomerization of  $\beta$ -methylstyrene.<sup>[40]</sup> The conversion obtained by using catalyst **5** was much lower in comparison to the other catalysts indicating that the structure of naphthol plays a significant role in isomerization.

It is known from the literature that azonaphthol/azonaphenyl-Ru complexes are used as catalysts for transfer hydrogenation of carbonyl compounds with 2-propanol as hydrogen source. In this classical pathway, the ruthenium complexes dehydrogenate the alcohol and deliver the hydrides to a ketone or an  $\alpha,\beta$ -unsaturated ketone.<sup>[41,42]</sup> However, the coordination of the substrate to the hydride ruthenium metal intermediate is not suitable here.

Moreover, studies by other teams dealing with metathesis reactions mediated by ruthenium-arene complexes have shown that the release of the arene ligand is crucial and is responsible for the generation of the catalytic active species.<sup>[43–45]</sup> Nonetheless, in this study, a careful NMR monitoring of the isomerization revealed no ligation of the cymene ligand (Figure 2). Comparing the <sup>1</sup>H NMR spectra of the cymene region of the catalyst before and during reaction (Figure 2), it was observed that the four doublet peaks of the cymene ring remain during the catalytic reaction. The shift of the peaks can be understood as a result of the transformation of coordination from  $\eta^6$  to  $\eta^4$ . Therefore, it is plausible to state that the proposed mechanism depicted in Scheme 4 is responsible for the formation of the catalytic active species during the isomerization reaction.

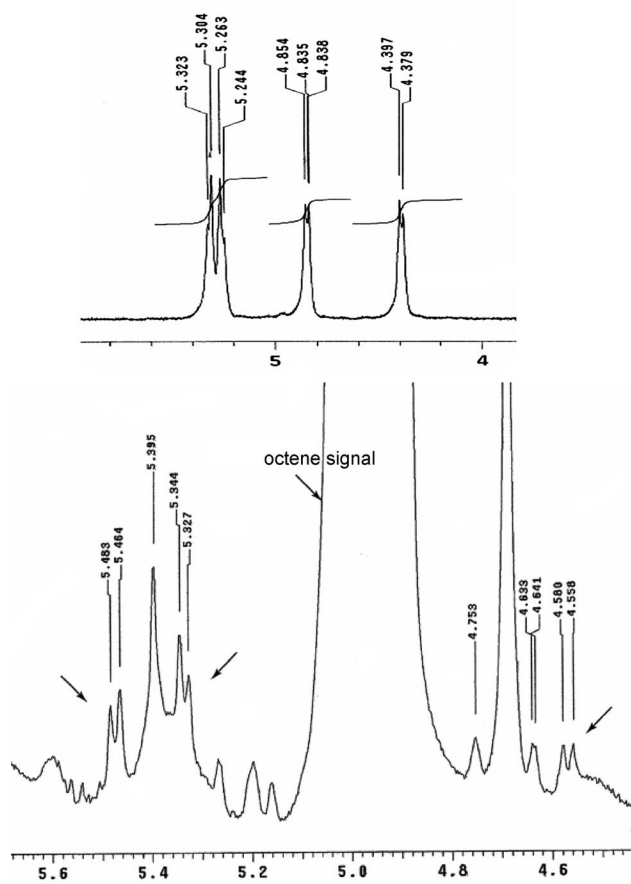
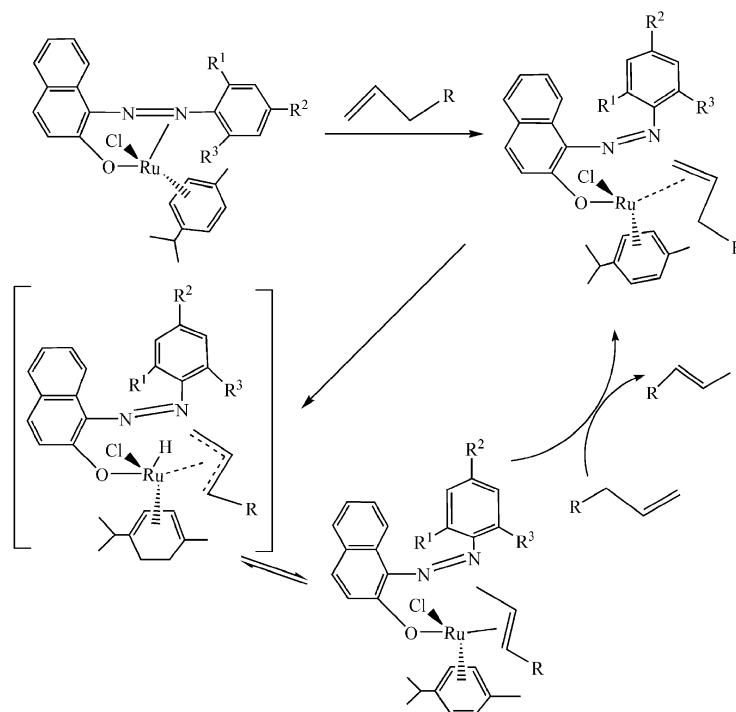


Figure 2. <sup>1</sup>H NMR spectrum of the cymene region of the catalyst before reaction (upper) and during reaction (bottom).



Scheme 4. Proposed mechanism for the isomerization using catalysts **1–5**.

The proposed pathway for this reaction is the decoordination of the nitrogen generating a vacant coordination site followed by the substrate coordination to the metal center. Subsequently, following the less common  $\pi$ -allyl mechanism, an oxidative addition of an activated allylic C–H bond to the metal yields a  $\pi$ -allyl metal hydride and generates the desired isomerization product.<sup>[46–50]</sup>

Furthermore, results obtained from experiments in which the influence of moisture and air sensitivity was studied proved that the isomerization using catalyst **1–5** is not affected and so, the isomerization can be executed using solvents from the bottle and in open air.

## Conclusions

In conclusion, a new class of ruthenium-based catalysts useful for isomerization has been synthesized. The X-ray crystal structure of the complex **4** reveals an octahedral environment around ruthenium. In contrast to what is observed for most other described catalysts, a noteworthy advantage of these catalysts is their inertness toward air and moisture preventing a meticulous pretreatment of solvents and substrates. This benefit makes the set-up of the experiment and the monitoring of the reaction progress very convenient.

The ruthenium complexes have been tested on their isomerization activity and their different behavior has been explained. Catalysts **1–4** are highly active for the isomerization without any dimerization or oligomerization. The obtained results imply that the naphthol moiety plays a significant role in the isomerization suggesting that the catalytic activity for 1-octene strongly depends on the steric and elec-

tronic environment of the ruthenium. So, the prospective of these catalysts in the field of isomerization can be further improved by fine-tuning of the ligand environment. The isomerization activity of complex **1** for allylbenzene is superior to most of the reported systems.<sup>[32,35,51–54]</sup>

In general, the results of the present exploration suggest a promising application of a new family of organoruthenium(II) complexes containing an azonaphthol/azophenyl group. Furthermore, the fact that these catalysts have been reported for transfer hydrogenation and exhibiting good isomerization activities (this work) allows them to combine these two methodologies to some interesting properties by using new substrate combinations. Further studies concerning these points are currently under investigation.

## Experimental Section

**General:** Unless otherwise stated, all reactions were carried out under a dry argon atmosphere following conventional Schlenk techniques. All solvents were distilled from the appropriate drying agents and deoxygenated prior to use. <sup>1</sup>H and <sup>13</sup>C NMR spectra were recorded on a Varian 300 spectrometer in CDCl<sub>3</sub> ( $\delta$  ppm). The NMR spectroscopic data suggest a 1:1 molar ratio of the *p*-cymene and the O,N ligand in **1–7**. Elemental analysis was performed using a Perkin–Elmer 2400 CHNS/O analyzer. The Sudan ligands were purchased from Aldrich and used as such; [(*p*-cymene)RuCl<sub>2</sub>]<sub>2</sub><sup>[55]</sup> and the ligands 1-(2,4,6-trimethylphenylazo)-2-naphthol,<sup>[56]</sup> (5-chloro-2-hydroxybenzenyl)(*p*-methylphenylazo)<sup>[57]</sup> were prepared according to the literature. All other chemicals used were of analytical grade without further purification.

Conversions, yields and selectivities of the isomerization reactions were obtained via capillary GC using a Finnigan Trace GC Ultra with an Ultra Fast Column Module (PH-5 5% diphenyl/95% di-

methyl poly-siloxane capillary, helium carrier gas, 1 mL/min column (10 m × 0.10 mm, 0.40 μm) and a FID detector. The temperature program starts at 50 °C increasing with 20 °C/min until the end temperature (255 °C) is reached.

**Isomerization Procedure:** Pretreatment of 1-octene was necessary before screening; it was passed through a column (20 cm × 1.5 cm) of neutral alumina (Acros, 50–200 μm) containing 15 g of alumina per 100 mL of 1-octene, collected in a Schlenk flask and degassed. In an empty 15 mL reaction vessel, an appropriate quantity of the catalyst under investigation was transferred together with toluene as solvent followed by the substrates. The vessel was immersed in an oil bath and allowed to equilibrate to the desired temperature before timing. Before GC-analysis, the reaction mixture was purified over a silica filter in order to remove the catalyst. Distilled, degassed hexane was used as solvent to prepare the GC samples and 1-dodecane was taken as internal standard.

**General Procedure for the Preparation of the Thallium Salts:** To a solution of the ligands 1–7 in dry THF (15 mL) was added dropwise a solution of thallium ethoxide in THF (5 mL) at room temperature. Immediately after the addition, a yellow solid formed and the reaction mixture was stirred for 2 h. Filtration of the solid under an Argon atmosphere gave the thallium salts in quantitative yields. The salts were used without further purification.

**General Procedure for the Preparation of [(η<sup>6</sup>-*p*-Cymene)RuCl(L<sup>*n*</sup>)] (1–7):** To a solution of [(η<sup>6</sup>-*p*-cymene)RuCl<sub>2</sub>]<sub>2</sub> (0.10 g, 0.16 mmol) in THF (5 mL) was added a solution of the corresponding appropriate thallium salt in THF (5 mL) and stirred for 6–8 h at room temperature. Thallium chloride was removed via filtration. After evaporation of the solvent, the residue was dissolved in a minimal amount of toluene and cooled to 0 °C. Hexane was used to precipitate the desired compound. The product was filtered, washed with hexane and dried in vacuo. The novel ruthenium complexes were obtained as red-brown to dark-brown solids; yields were between 90–98%.

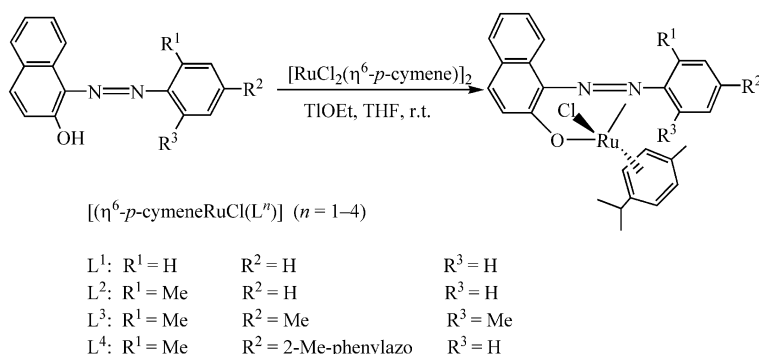
**[(η<sup>6</sup>-*p*-Cymene)RuCl(L<sup>1</sup>)] (1):** (Scheme 5) Although this complex has been reported by Rakesh et al.,<sup>[17]</sup> a modified procedure was used to get high yield: 96% of a red-brown powder. C<sub>26</sub>H<sub>25</sub>ClN<sub>2</sub>ORu (518.02): calcd. C 60.28, H 4.87, N 5.41; found C 59.95, H 4.47, N 5.13. IR:  $\tilde{\nu} = \nu_{\text{N=N}}$  1371.63,  $\nu_{\text{C-O-Ru}}$  1312.31 cm<sup>-1</sup>. <sup>1</sup>H NMR:  $\delta$  = 1.05, 1.12 (2d, *J*<sub>HH</sub> = 7 Hz, 2 × 3 H, 2 CH<sub>3</sub>, isopropyl of *p*-cymene), 2.25 (s, 3 H, CH<sub>3</sub>, *p*-cymene), 2.56 (sp, *J*<sub>HH</sub> = 7 Hz, 1 H, CH, isopropyl), 4.59, 4.96 (2d, *J*<sub>HH</sub> = 6 Hz, 2 × 1 H, ring H of *p*-cymene), 5.40 (s, 2 H, ring H of *p*-cymene), 7.14–7.56 (m, 7 H, ring H), 7.67 (d, *J*<sub>HH</sub> = 9 Hz, 1 H, naphthol ring H), 7.90 (d, *J*<sub>HH</sub> = 7 Hz, 2 H, naphthol ring H), 8.26 (d, *J*<sub>HH</sub> = 8 Hz, 1 H, naphthol ring H) ppm. <sup>13</sup>C NMR:  $\delta$  = 18.79 (CH, isopropyl), 21.89, 22.72 (2 CH<sub>3</sub>, isopropyl), 30.50 (Me, *p*-cymene), 83.41, 83.72, 85.83, 88.08, 101.14, 101.80

(ring of *p*-cymene), 121.95, 123.46, 124.49, 124.79, 127.19, 127.64, 127.71, 127.77, 128.28, 130.11, 134.89, 137.26, 153.12 (C–L<sup>1</sup>), 162.29 (C next to O) ppm.

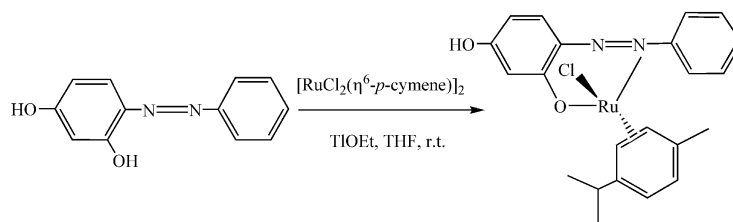
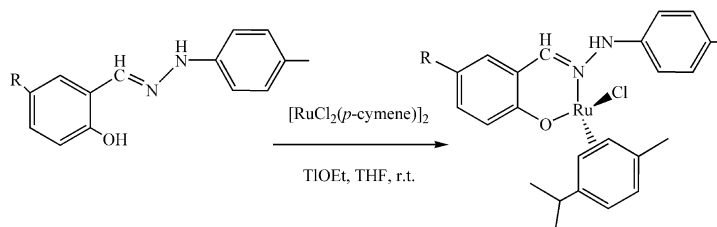
**[(η<sup>6</sup>-*p*-Cymene)RuCl(L<sup>2</sup>)] (2):** (Scheme 5) Yield 93%, red-brown powder. C<sub>28</sub>H<sub>29</sub>ClN<sub>2</sub>ORu (546.07): calcd. C 61.58, H 5.36, N 5.13; found C 62.01, H 5.81, N 5.34. IR:  $\tilde{\nu} = \nu_{\text{N=N}}$  1372.15 cm<sup>-1</sup>,  $\nu_{\text{C-O-Ru}}$  1310.99 cm<sup>-1</sup>. <sup>1</sup>H NMR:  $\delta$  = 1.12, 1.24 (2d, *J*<sub>HH</sub> = 7 Hz, 2 × 3 H, 2 CH<sub>3</sub>, isopropyl of *p*-cymene), 2.16 (s, 3 H, CH<sub>3</sub>-phenyl), 2.33 (s, 3 H, CH<sub>3</sub>-phenyl), 2.44 (s, 3 H, CH<sub>3</sub>, *p*-cymene), 2.64 (sp, 1 H, CH, isopropyl), 4.31 (s, 1 H, ring H of *p*-cymene), 5.02 (s, 1 H, ring H of *p*-cymene), 5.38, 5.45 (2d, *J*<sub>HH</sub> = 21 Hz, 2 × 1 H, ring H of *p*-cymene), 7.13–7.21 (m, 4 H, ring H), 7.32 (d, *J*<sub>HH</sub> = 6.9 Hz, 1 H, naphthol ring H), 7.51 (d, *J*<sub>HH</sub> = 7.8 Hz, 1 H, naphthol ring H), 7.64 (d, *J*<sub>HH</sub> = 9.3 Hz, 1 H, naphthol ring H), 7.93 (d, *J*<sub>HH</sub> = 9 Hz, 1 H, naphthol ring H), 8.13 (d, *J*<sub>HH</sub> = 8.4 Hz, 1 H, naphthol ring H) ppm. <sup>13</sup>C NMR:  $\delta$  = 18.94 (CH, isopropyl), 22.15, 22.45 (2 CH<sub>3</sub>, isopropyl), 27.23 (CH<sub>3</sub>-phenyl), 30.63 (Me, *p*-cymene), 31.51 (CH<sub>3</sub>-phenyl), 77.94, 78.71, 80.51, 81.30 (ring of *p*-cymene), 121.92, 123.43, 124.31, 125.66, 127.79, 128.67, 128.91, 129.67, 133.48, 134.89, 153.67 (C–L<sup>2</sup>), 162.24 (C next to O) ppm.

**[(η<sup>6</sup>-*p*-Cymene)RuCl(L<sup>3</sup>)] (3):** (Scheme 5) Yield 95%, red-brown powder. C<sub>29</sub>H<sub>31</sub>ClN<sub>2</sub>ORu (560.10): calcd. C 62.18, H 5.59, N 5.00; found C 61.77, H 5.16, N 4.77. IR:  $\tilde{\nu} = \nu_{\text{N=N}}$  1376.87 cm<sup>-1</sup>,  $\nu_{\text{C-O-Ru}}$  1308.22 cm<sup>-1</sup>. <sup>1</sup>H NMR:  $\delta$  = 1.26, 1.35 (2d, *J*<sub>HH</sub> = 7 Hz, 2 × 3 H, 2 CH<sub>3</sub>, isopropyl of *p*-cymene), 2.03, 2.06 (s, 2 × 3 H, 2 CH<sub>3</sub>-phenyl), 2.28 (s, 3 H, CH<sub>3</sub>-phenyl), 2.60 (s, 3 H, CH<sub>3</sub>, *p*-cymene), 2.75 (sp, 1 H, CH, isopropyl), 4.46, 4.91 (s, 2 × 1 H, ring H of *p*-cymene), 5.33, 5.38 (d, *J*<sub>HH</sub> = 7 Hz, 2 × 1 H, ring H of *p*-cymene), 6.96–7.17 (m, 5 H, ring H), 7.49 (d, *J*<sub>HH</sub> = 9 Hz, naphthol ring H), 7.58 (d, *J*<sub>HH</sub> = 7 Hz, naphthol ring H), 7.95 (d, *J*<sub>HH</sub> = 8 Hz, naphthol ring H) ppm. <sup>13</sup>C NMR:  $\delta$  = 17.68, 18.02 (2 CH<sub>3</sub>-phenyl), 19.08 (CH, isopropyl), 20.98 (CH<sub>3</sub>-phenyl), 22.09, 22.53 (2 CH<sub>3</sub>, isopropyl), 30.92 (Me, *p*-cymene), 79.40, 83.67, 87.31, 91.33 (ring of *p*-cymene), 121.91, 123.37, 124.14, 127.54, 127.69, 128.46, 129.47, 130.48, 130.88, 136.84, 154.70 (C–L<sup>3</sup>), 162.23 (C next to O) ppm.

**[(η<sup>6</sup>-*p*-Cymene)RuCl(L<sup>4</sup>)] (4):** (Scheme 5) Yield 93%, red-brown powder. C<sub>34</sub>H<sub>33</sub>ClN<sub>4</sub>ORu (650.19): calcd. C 62.80, H 5.13, N 8.62; found C 62.57, H 5.24, N 8.23. IR:  $\tilde{\nu} = \nu_{\text{N=N}}$  1370.93 cm<sup>-1</sup>,  $\nu_{\text{C-O-Ru}}$  1294.59 cm<sup>-1</sup>. <sup>1</sup>H NMR:  $\delta$  = 1.13, 1.26 (2d, *J*<sub>HH</sub> = 6.6 Hz, 2 × 3 H, 2 CH<sub>3</sub>, isopropyl of *p*-cymene), 2.20, 2.49 (s, 2 × 3 H, 2 CH<sub>3</sub>-phenyl), 2.96 (s, 3 H, CH<sub>3</sub>, *p*-cymene), 3.90 (sp, 1 H, CH, isopropyl), 4.43, 5.01 (s, 2 × 1 H, ring H of *p*-cymene), 5.42, 5.51 (d, *J*<sub>HH</sub> = 5.7 Hz, 2 × 1 H, ring H of *p*-cymene), 7.20–7.40 (m, 8 H, ring H), 7.53 (d, *J*<sub>HH</sub> = 6 Hz, naphthol ring H), 7.56 (d, *J*<sub>HH</sub> = 9 Hz, naphthol ring H), 7.93 (d, *J*<sub>HH</sub> = 6.6 Hz, naphthol ring H), 8.14 (d, *J*<sub>HH</sub> = 6.4 Hz, naphthol ring H), 8.25 (d, *J*<sub>HH</sub> = 7 Hz, naphthol ring H) ppm. <sup>13</sup>C NMR:  $\delta$  = 17.63 (CH, isopropyl), 18.32,



Scheme 5. Synthesis procedure for catalysts 1–4.

Scheme 6. Synthesis procedure for catalyst **5**.Scheme 7. Synthesis procedure for catalysts **6** and **7**.

18.43 (2 CH<sub>3</sub>-phenyl), 21.52, 22.89 (2 CH<sub>3</sub>, isopropyl), 30.60 (Me, *p*-cymene), 79.68, 80.60, 83.29, 86.71, 87.69, 89.09 (ring of *p*-cymene), 115.31, 121.09, 121.64, 121.95, 122.75, 123.58, 123.78, 124.31, 124.58, 125.20, 126.51, 127.19, 127.85, 128.917, 130.40, 131.23, 131.39, 134.69, 136.744, 137.76, 151.26 (C-L<sup>5</sup>), 161.77 (C next to O) ppm.

**[(η<sup>6</sup>-*p*-Cymene)RuCl(L<sup>5</sup>)] (5):** (Scheme 6) Yield 90%, red-brown powder. C<sub>22</sub>H<sub>23</sub>ClN<sub>2</sub>O<sub>2</sub>Ru (483.96): calcd. C 54.60, H 4.80, N 5.79; found C 55.02, H 4.99, N 5.44. IR:  $\tilde{\nu} = \nu_{\text{N=N}}$  1364.14 cm<sup>-1</sup>,  $\nu_{\text{C-O-Ru}}$  1278.24 cm<sup>-1</sup>. <sup>1</sup>H NMR:  $\delta$  = 1.24, 1.97 (2d,  $J_{\text{HH}}$  = 4.5 Hz, 2 × 3 H, 2 CH<sub>3</sub>, isopropyl of *p*-cymene), 2.18 (s, 3 H, CH<sub>3</sub>, *p*-cymene), 2.32 (sp, 1 H, CH, isopropyl), 4.60 (s, 2 H, ring H of *p*-cymene), 4.99, 5.20 (d,  $J_{\text{HH}}$  = 6 Hz, 2 × 1 H, ring H of *p*-cymene), 6.91, 7.00 (d,  $J_{\text{HH}}$  = 9 Hz, 2 × 1 H, ring H), 7.12 (s, 1 H, ring H), 7.23–7.42 (m, 5 H, ring H), 9.79 (s, H of hydroxy) ppm. <sup>13</sup>C NMR:  $\delta$  = 18.01 (CH, isopropyl), 22.85, 23.67 (2 CH<sub>3</sub>, isopropyl), 31.15 (Me, *p*-cymene), 79.88, 81.91, 83.30, 84.34, 97.18, 98.56 (ring of *p*-cymene), 113.54, 121.46, 123.57, 127.72, 135.07, 140.01, 146.94, 152.26, 156.36, 165.36, (C next to O) ppm.

**[(η<sup>6</sup>-*p*-Cymene)RuCl(L<sup>6</sup>)] (6):** (Scheme 7) Yield 92%, red-brown powder. C<sub>24</sub>H<sub>27</sub>ClN<sub>2</sub>ORu (496.01): calcd. C 58.12, H 5.49, N 5.65; found C 58.38, H 5.48, N 5.46. IR:  $\tilde{\nu} = \nu_{\text{N=N}}$  1377.76 cm<sup>-1</sup>,  $\nu_{\text{C-O-Ru}}$  1278.21 cm<sup>-1</sup>. <sup>1</sup>H NMR:  $\delta$  = 1.13, 1.22 (d,  $J_{\text{HH}}$  = 1.2 Hz, 2 × 3 H, 2 CH<sub>3</sub>, isopropyl of *p*-cymene), 2.28 (s, 3 H, CH<sub>3</sub>, *p*-cymene), 2.37 (s, 3 H, CH<sub>3</sub>-phenyl), 2.77 (sp, 1 H, CH, isopropyl), 4.96, 5.17 (s, 2 × 1 H, ring H of *p*-cymene), 5.28, 5.45 (d,  $J_{\text{HH}}$  = 6 Hz, 2 × 1 H, ring H of *p*-cymene), 6.48–7.85 (m, 8 H, ring H) ppm. <sup>13</sup>C NMR:  $\delta$  = 17.48 (CH<sub>3</sub>-phenyl), 18.62 (CH, isopropyl), 22.64, 23.40 (2 CH<sub>3</sub>, isopropyl), 29.71 (Me, *p*-cymene), 65.45 (–CH=N=N), 81.52, 82.56, 85.74, 86.17 (ring of *p*-cymene), 113.09, 115.34, 121.28, 123.79, 128.23, 131.30, 132.43, 135.28, 160.85, 161.76 (C next to O) ppm.

**[(η<sup>6</sup>-*p*-Cymene)RuCl(L<sup>7</sup>)] (7):** (Scheme 7) Yield 91%, red-brown powder. C<sub>24</sub>H<sub>26</sub>Cl<sub>2</sub>N<sub>2</sub>ORu (530.46): calcd. C 54.34, H 4.95, N 5.28; found C 54.73, H 4.59, N 5.49. IR:  $\tilde{\nu} = \nu_{\text{N=N}}$  1380.96 cm<sup>-1</sup>,  $\nu_{\text{C-O-Ru}}$  1293.15 cm<sup>-1</sup>. <sup>1</sup>H NMR:  $\delta$  = 1.25, 1.32 (d,  $J_{\text{HH}}$  = 6 Hz, 2 × 3 H, 2 CH<sub>3</sub>, isopropyl of *p*-cymene), 1.86 (s, 3 H, CH<sub>3</sub>, *p*-cymene), 2.17 (sp, 1 H, CH, isopropyl), 2.36 (s, 3 H, CH<sub>3</sub>-phenyl), 3.75 (s, 2 × 1 H, ring H of *p*-cymene), 4.77, 5.23 (d,  $J_{\text{HH}}$  = 3.6 Hz, 2 × 1 H, ring H of *p*-cymene), 7.18–7.36 (m, 9 H, ring H) ppm. <sup>13</sup>C NMR:  $\delta$  = 18.42 (CH<sub>3</sub>-phenyl), 18.94 (CH, isopropyl), 21.65,

22.99 (2 CH<sub>3</sub>, isopropyl), 30.60 (Me, *p*-cymene), 66.54 (–CH=N=N), 80.52, 81.31, 83.21, 88.09 (ring of *p*-cymene), 114.02, 118.05, 122.34, 129.37, 129.82, 134.738, 135.14, 136.23, 164.16, 165.33 (C next to O) ppm.

**Procedure for the Preparation of HL<sup>3</sup>:** (Scheme 1) 7.3 g (54 mmol) of 2,4,6-trimethyl aniline is dissolved in a solution containing 16 mL of concd. hydrochloric acid and 16 mL of water. By addition of a solution of 4.0 g sodium nitrite in 20 mL water in small portions and keeping the solution below 10 °C diazotizing occurs. The temperature is kept below 10 °C until the colour of potassium iodide–starch paper dipped into the solution immediately turns blue. A cooled solution (5 °C) of 7.8 g β-naphthol in 45 mL of 10% sodium hydroxide solution is vigorously stirred and added very slowly to the cold diazonium salt solution. A red color appears and red crystals of 1-(2,4,6-trimethylphenylazo)-2-naphthol (Scheme 1) precipitate. The filtered product was recrystallized from glacial acetic acid, yielding 26% of HL<sup>3</sup>. C<sub>19</sub>H<sub>18</sub>N<sub>2</sub>O (290.36): calcd. C 78.58, H 6.26, N 9.65; found C 78.20, H 5.95, N 9.31. <sup>1</sup>H NMR:  $\delta$  = 2.35 (s, 3 H, CH<sub>3</sub>), 2.601 (s, 6 H, 2 CH<sub>3</sub>), 6.92 (s, 1 H, naphthol ring H), 6.95 (s, 1 H, naphthol ring H), 7.00 (s, 2 H, phenyl ring H), 7.47 (t,  $J$  = 7.5 Hz, 1 H, naphthol ring H), 7.63 (t,  $J$  = 7.2 Hz, 1 H, naphthol ring H), 7.24 (d,  $J$  = 6.6 Hz, 1 H, naphthol ring H), 7.82 (d,  $J$  = 9.6 Hz, 1 H, naphthol ring H), 8.41 (d,  $J$  = 6.6 Hz, 1 H, hydroxy) ppm.

**Procedure for the Preparation of HL<sup>6</sup>:** Triethylamine (4 equiv. 25.2 mmol) is added to a 50 mL methanol solution of the appropriate tolylhydrazine hydrochloride (1 equiv., 6.3 mmol) resulting in a bright yellow solution followed by a dropwise addition of a 10 mL methanol solution of salicylaldehyde (1 equiv., 6.3 mmol). An orange-yellow solution is obtained after 5–6 h stirring at room temperature. Thereafter the solvent was evaporated till precipitation occurred. (Scheme 1). Filtering the solid and recrystallization using ethyl acetate/hexane (1:8) yielded 38% of HL<sup>6</sup>. C<sub>14</sub>H<sub>14</sub>N<sub>2</sub>O (226.28): calcd. C 74.30, H 6.25, N 12.38; found C 74.48, H 6.52, N 12.01. <sup>1</sup>H NMR:  $\delta$  = 2.29 (s, 3 H, CH<sub>3</sub>), 6.86–7.25 (aromatic ring, 4 H, m), 7.40 (m, 3 H, NH), 7.82 (s, 1 H, CH), 10.91 (s, 1 H, OH) ppm.

**Procedure for the Preparation of HL<sup>7</sup>:** (Scheme 1) The same procedure was used as for HL<sup>6</sup> except that 5-chlorosalicylaldehyde was applied instead of salicylaldehyde. The yield after recrystallization was 39%. C<sub>14</sub>H<sub>13</sub>ClN<sub>2</sub>O (260.72): calcd. C 64.49, H 5.04, N 10.75; found C 64.11, H 4.97, N 10.31. <sup>1</sup>H NMR:  $\delta$  = 2.30 (s, 3 H), 6.905

(aromatic ring, 1 H, s), 7.10 (aromatic ring, 1 H, s), 7.26 (aromatic ring, 1 H, s), 7.51 (s, 1 H, NH), 7.75 (s, 1 H, CH), 10.85 (s, 1 H, OH) ppm.

**General Procedure for the Catalytic Testing:** A mixture of one of the catalysts 1–7 and the appropriate amount of substrate (1-octene or allylbenzene) was dissolved in toluene (1 mL) and heated to the desired temperature for 12 h. After the reaction time, the mixture was cooled to room temperature. The catalyst was removed by addition of 2 mL of hexane followed by filtration through a silica filter.

CCDC-719359 contains the supplementary crystallographic data for this paper. These data can be obtained free of charge from The Cambridge Crystallographic Data Centre via [www.ccdc.cam.ac.uk/data\\_request/cif](http://www.ccdc.cam.ac.uk/data_request/cif).

## Acknowledgments

F. D. is indebted to the BOF (Bijzonder Onderzoeksfonds) of Ghent University for a research grant. F. V. is indebted to the FWO Flanders (Fonds voor Wetenschappelijk Onderzoek, Vlaanderen) and Ghent University for financial support.

- [1] W. A. Herrmann, *Applied Homogeneous Catalysis with Organometallic Compounds*, **2002**, 2<sup>nd</sup> ed., vol. 3, p. 980–991.
- [2] G. J. Boons, A. Burton, S. Isles, *Chem. Commun.* **1996**, 141–142.
- [3] B. Therrien, *Eur. J. Inorg. Chem.* **2009**, 17, 2445–2453.
- [4] H. Werner, *Organometallics* **2005**, 24, 1036–1049.
- [5] I. Ozdemir, S. Demir, B. Cetinkaya, C. Gourlaouen, F. Maseras, C. Bruneau, P. H. Dixneuf, *J. Am. Chem. Soc.* **2008**, 130, 1156–1157.
- [6] X. Sauvage, Y. Borguet, G. Zaragoza, A. Demonceau, L. Delaude, *Adv. Synth. Catal.* **2009**, 351, 441–455.
- [7] C. Standfest-Hauser, C. Slugovc, K. Mereiter, R. Schmid, K. Kirchner, L. Xiao, W. Weissensteiner, *J. Chem. Soc., Dalton Trans.* **2001**, 2989–2995.
- [8] M. J. L. Tschan, G. Süß-Fink, F. Cherioux, B. Therrien, *Chem. Eur. J.* **2007**, 13, 292–299.
- [9] Y. Chen, Y. H. Tang, S. B. Liu, M. Lei, W. H. Fang, *Organometallics* **2009**, 28, 2078–2084.
- [10] K. Everaere, A. Mortreux, J. F. Carpentier, *Adv. Synth. Catal.* **2003**, 345, 67–77.
- [11] D. A. Alonso, P. Brandt, S. J. M. Nordin, P. G. Andersson, *J. Am. Chem. Soc.* **1999**, 121, 9580–9588.
- [12] B. De Clercq, F. Verpoort, *Tetrahedron Lett.* **2001**, 42, 8959–8963.
- [13] X. Sauvage, Y. Borguet, A. F. Noels, L. Delaude, A. Demonceau, *Adv. Synth. Catal.* **2007**, 349, 255–265.
- [14] R. Castarlenas, C. Vovard, C. Fischmeister, P. H. Dixneuf, *J. Am. Chem. Soc.* **2006**, 128, 4079–4089.
- [15] F. Ding, Y. G. Sun, S. Monsaert, R. Drozdak, I. Dragutan, V. Dragutan, F. Verpoort, *Curr. Org. Synth.* **2008**, 5, 291–304.
- [16] I. Omae, *Chem. Rev.* **1979**, 79, 287–321.
- [17] R. K. Rath, M. Nethaji, A. R. Chakravarty, *J. Organomet. Chem.* **2001**, 633, 79–84.
- [18] S. M. P. Kanchana Suia, S. Bhattacharya, *Polyhedron* **1999**, 18, 631–640.
- [19] S. Kannan, R. Ramesh, *Polyhedron* **2006**, 25, 3095–3103.
- [20] S. Kannan, R. Ramesh, Y. Liu, *J. Organomet. Chem.* **2007**, 692, 3380–3391.
- [21] J. Hannedouche, G. J. Clarkson, M. Wills, *J. Am. Chem. Soc.* **2004**, 126, 986–987.
- [22] J. S. M. Samec, A. H. Ell, J. B. Aberg, T. Privalov, L. Eriksson, J. E. Backvall, *J. Am. Chem. Soc.* **2006**, 128, 14293–14305.
- [23] J. S. M. Samec, A. H. Ell, J. E. Backvall, *Chem. Commun.* **2004**, 2748–2749.
- [24] C. G. Hartung, C. Breindl, A. Tillack, M. Beller, *Tetrahedron* **2000**, 56, 5157–5162.
- [25] W. Herrmann, B. Cornils, *Applied Homogeneous Catalysis with Organometallic Compounds* **1996**, vol. 2, p. 980–991.
- [26] G. W. Parshall, S. D. Tittel, *Homogeneous Catal.* **1992**, 9–24.
- [27] B. Mondal, M. G. Walawalkar, G. K. Lahiri, *J. Chem. Soc., Dalton Trans.* **2000**, 4209–4217.
- [28] C. Averbuj, M. S. Eisen, *J. Am. Chem. Soc.* **1999**, 121, 8755–8759.
- [29] W. E. McCormack, M. Orchin, *J. Organomet. Chem.* **1977**, 129, 127–137.
- [30] H. Sertchook, D. Avnir, J. Blum, F. Joo, A. Katho, H. Schumann, R. Weimann, S. Wernik, *J. Mol. Catal. A* **1996**, 108, 153–160.
- [31] M. Setty Fichman, Y. Sasson, J. Blum, *J. Mol. Catal. A* **1997**, 126, 27–36.
- [32] A. C. Cooper, K. G. Caulton, *Inorg. Chim. Acta* **1996**, 251, 41–51.
- [33] V. V. Smirnov, S. A. Nikolaev, G. P. Murav'eva, L. A. Tyurina, A. Y. Vasil'kov, *Kinet. Catal.* **2007**, 48, 265–270.
- [34] S. Lachaize, A. Caballero, L. Vendier, S. Sabo-Etienne, *Organometallics* **2007**, 26, 3713–3721.
- [35] S. Krompiec, N. Kuznik, M. Urbala, J. Rzepa, *J. Mol. Catal. A* **2006**, 248, 198–209.
- [36] E. O. Sherman, M. Olson, *J. Organomet. Chem.* **1979**, 172, C13–C19.
- [37] S. Krompiec, J. Suwinski, R. Grobelny, *J. Mol. Catal. A* **1994**, 89, 303–316.
- [38] M. A. Aramendia, V. Borau, C. Jimenez, A. Marinas, J. M. Marinas, F. J. Urbano, *J. Mol. Catal. A* **2002**, 182–183, 25–34.
- [39] Z. K. Yu, S. G. Yan, G. T. Zhang, W. He, L. D. Wang, Y. Li, F. L. Zeng, *Adv. Synth. Catal.* **2006**, 348, 111–117.
- [40] R. H. Crabtree, *The Organometallic Chemistry of the Transition Metals*, chapter 9, **1988**, p. 188–190.
- [41] R. Noyori, *Angew. Chem. Int. Ed.* **2002**, 41, 2008–2022.
- [42] R. L. Chowdhury, J.-E. Bäckvall, *J. Chem. Soc., Chem. Commun.* **1991**, 1063–1063.
- [43] B. De Clercq, F. Verpoort, *J. Mol. Catal. A* **2002**, 180, 67–76.
- [44] J. A. S. Howell, N. F. Ashford, D. T. Dixon, J. C. Kola, T. A. Albright, S. K. Kang, *Organometallics* **1991**, 10, 1852–1864.
- [45] L. Ackermann, A. Fürstner, T. Weskamp, F. J. Kohl, W. A. Herrmann, *Tetrahedron Lett.* **1999**, 40, 4787–4790.
- [46] G. W. Parshall, *Homogeneous Catalysis*, Wiley-VCH, Weinheim, Germany, **1980**, p. 31–35.
- [47] R. H. Crabtree, *The Organometallic Chemistry of the Transition Metals*, Wiley, New York, **1988**, p. 188–190.
- [48] D. V. McGrath, R. H. Grubbs, *Organometallics* **1994**, 13, 224–235.
- [49] S. K. Sharma, V. K. Srivastava, R. V. Jasra, *J. Mol. Catal. A* **2006**, 245, 200–209.
- [50] S. Krompiec, M. Krompiec, R. Penczek, H. Ignasiak, *Coord. Chem. Rev.* **2008**, 252, 1819–1841.
- [51] E. Shaviv, M. Botoshansky, M. S. Eisen, *J. Organomet. Chem.* **2003**, 683, 165–180.
- [52] W. Wu, J. G. Verkade, *Arkivoc* **2004**, 88–95.
- [53] O. Kuhl, T. Koch, F. B. Somoza, P. C. Junk, E. Hey-Hawkins, D. Plat, M. S. Eisen, *J. Organomet. Chem.* **2000**, 604, 116–125.
- [54] A. M. Trzeciak, J. J. Ziolkowski, *J. Organomet. Chem.* **2000**, 597, 69–76.
- [55] M. A. Bennett, T. N. Huang, T. W. Matheson, A. K. Smith, *Inorg. Synth.* **1982**, 21, 74–75.
- [56] D. I. McIsaac, C. M. V. Stephen, J. Geier, A. Decken, S. A. Westcott, *Inorg. Chim. Acta* **2006**, 359, 2771–2779.
- [57] H. Z. Alkathlan, *Tetrahedron* **2003**, 59, 8163–8170.
- [58] M. B. Dinger, J. C. Mol, *Organometallics* **2003**, 22, 1089–1095.

Received: September 16, 2009

Published Online: February 22, 2010